Solid Lipid Nanoparticles (SLNs) with Potential as Cosmetic Hair Formulations Made from Otoba Wax and Ultrahigh Pressure Homogenization

Sandra Rubiano [1], Juan D. Echeverri [1,2] and Constain H. Salamanca [1,2,3,*]

[1]   Programa de Maestría en Formulación de Productos Químicos y Derivados, Facultad de Ciencias Naturales, Universidad Icesi, Calle 18 No. 122–135, Cali 76003, Colombia; srubiano155@gmail.com (S.R.); juandiegoqf@hotmail.com (J.D.E.)

[2]   Laboratorio de Diseño y Formulación de Productos Químicos y Derivados, Departamento de Ciencias Farmacéuticas, Facultad de Ciencias Naturales, Universidad Icesi, Calle 18 No. 122–135, Cali 76003, Colombia

[3]   Centro de Ingredientes Naturales Especializados y Biotecnológicos (CINEB), Facultad de Ciencias Naturales, Universidad Icesi, Calle 18 No. 122–135, Cali 76003, Colombia

*   Correspondence: chsm70@gmail.com or chsalamanca@icesi.edu

Abstract: The development and physicochemical characterization of solid lipid nanoparticles (SLNs) with potential for formulating hair cosmetic products were carried out. SLNs were made from Otoba wax, which is native to the tropical Andean region and has a high chemical composition of fatty acids with intermediate chains. SLNs were formulated by preparing wax-in-water dispersions at two internal phase proportions (low = 5% *w/w* and high = 20% *w/w*), using the same ratio of surfactant system and preservatives. The coarse dispersions were subjected to ultrahigh pressure homogenization (UHPH), and thermal stability assays for 4 weeks were carried out, where changes in Creaming Index, droplet size, polydispersity, viscosity, zeta potential, conductivity, and pH were evaluated. The results showed that Otoba wax has a required HLB value around 9 and is mainly composed of lauric (~35%) and myristic (~45%), which have been reported to improve the condition of hair loss. Regarding the development on SLNs, it was found that the internal phase concentration did not considerably affect the physicochemical and microbiological properties. Likewise, it was found that UHPH enabled the production of SLNs with particle sizes <200 nm, low polydispersity (<0.3), high zeta potential values, and suitable physical and microbiological stability. Therefore, Otoba wax has potential for the development of SLNs applicable to cosmetic formulations, especially for hair products.

Keywords: hair cosmetic formulations; Otoba wax; solid lipid nanoparticles (SLNs), thermal stability assay; ultrahigh pressure homogenization (UHPH)

1. Introduction

Solid lipid nanoparticles (SLNs) are spherical systems with sizes ranging between 50 and 1000 nm and consist of a solid core made of purified triglyceride blends or waxes that solidify at temperatures between 25 °C and 37 °C [1]. SLNs in aqueous medium usually exhibit a similar behavior to that shown by conventional emulsions; therefore, their formulations employ surfactants for stabilization [2]. Likewise, SLNs are mostly developed through processes that combine many methodologies. The first method involves the heating of the waxes to temperatures above their respective melting point, followed by the development of emulsions by conventional procedures [3]. Once the emulsions have been made, they are subjected to some high energy technique (top-down type), such as conventional dispersion by homomixer, colloid mills, ultrasound, or high and ultrahigh pressure homogenization (UHPH) [4–6].

UHPH is a technique based on a high-energy dispersion process in which a conventional dispersion (coarse size) is passed through a micrometer diameter nozzle, which causes high turbulence, shear, and cavitation [7]. Consequently, UHPH allows dispersed systems to achieve droplet sizes between 10 and 500 nm with very low polydispersity, considerably increasing physical stability. Therefore, when the nanoemulsified system is cooled, it is transformed into a suspension in which the dispersed phase corresponds to solid, spherical, and nanometric particles with a lipid core surrounded by a compact stabilizing layer of surfactants.

Like other nanometric vehicle systems, SLNs contain several advantages and disadvantages; therefore, it is necessary to consider each aspect before embarking on a potential formulation for cosmetic products. For instance, these nanoparticle systems are considered to exhibit high biocompatibility and low toxicity because they are primarily made of biodegradable compounds [8]. Likewise, such systems are considered eco-friendly alternatives for the development of several types of products, because they allow the solubilization and vehiculization of a variety of nonpolar compounds, allowing manufacturers to forego the use of organic solvents during the manufacturing process or in the product itself [9]. Furthermore, these nanosystems have been widely regarded for their ability to act as slow and controlled release systems for active ingredients, describing similar release mechanisms to those shown by other analog nanoparticles, such as liposomes and polymeric nanoparticles [10–13]. Finally, SLNs may be obtained using scalable "top-down" methodologies, which is an important factor to consider for the development of products with industrial potential [14]. By contrast, several disadvantages have also been described for these nanosystems, such as problems related to changes in the morphological structure inside the lipidic core and problems in the release of the ingredients incorporated therein. For instance, it is necessary to melt the waxy components during the process of incorporating compounds inside the lipidic core, and this process can lead to subsequent changes in the internal lipid structure. These changes may result in the formation of different polymorphs, which may also promote other changes in physicochemical properties such as solubility and permeability. Likewise, the solid lipidic core of these nanoparticles has very high viscosity, which considerably affects the diffusion process of ingredients and the release mechanism [3,6,8].

In recent decades, SLNs have shown to be promising alternatives for several sectors, such as in pharmaceuticals [11,12,15], foodstuff [16], cosmetics, and personal care [17,18]. The pharmaceutical industry contains the largest number of reports and applications. However, for the cosmetic and personal care products sector, SLNs could represent an interesting alternative for the development of innovative products. For instance, these nanoparticulate systems can provide a series of advantages that are usually difficult to achieve with conventional formulations. Some of these benefits correspond to the controlled release of ingredients such as fragrances or antiaging compounds, making them last longer or be more effective. This would be even more advantageous if the raw materials used could also exert a cosmetic effect, in addition to forming nanometric vehicles. In this context, Otoba wax has a significant potential as a multifunctional cosmetic raw material because it includes both the features. This wax is composed primarily of intermediate chain fatty acids (lauric and myristic) and exhibits a low melting point at approximately 34 °C [19]. Furthermore, Otoba wax has several ethnobotanical properties that exert positive effects on the skin.

According to the ethnobotanical properties described in several countries of the tropical Andean region (Panama, Colombia, Peru, and Ecuador), this wax could strengthen and grow hairs, as well as it recovers some skin conditions in farm animals. Otoba wax, which is currently marketed in these Andean countries as raw material or as an exotic product for hair treatment, is obtained from the seeds of several plants belonging to the *Myristicaceae* family. According to López et al. [20], this family consist of approximately 20 species distributed in four plant genera corresponding to *Iryanthera* (35%), *Osteophloeum* (5%), *Otoba* (5%), and *Virola* (55%).

Although Otoba wax is already being marketed, information is limited on this compound. For instance, the extraction process is unclear, and the methodologies employed are usually rustic, unsophisticated, technically limited, and not standardized. Furthermore, it is unclear whether all

species in this family produce Otoba waxes that have similar chemical compositions or whether the wax is obtained from a random mixture of seeds from different species of this family. Similarly, it seems that this wax is extracted from native plants, which may further address to a variability in their chemical quality and consistency in each production batch. It is well known that plants can change their primary and secondary metabolite compositions depending on the environmental conditions. Consequently, the weather, thermal floor, and hours of light shade, as well as the type, quality, and quantity of nutrients present in the soil may affect these proportions and the chemical composition obtained for use. This study focused on the technical aspects of producing Otoba wax, which has enormous potential as an exotic and multifunctional raw material for the cosmetic sector. For this, the study focused to (i) characterize the chemical composition of Otoba wax commercialized as a raw material by following standardized and widely recognized methods, (ii) determine the required HLB value by using thermodynamic surface (contact angle) and Creaming Index tests, and (iii) develop, characterize, and evaluate the physical and microbiological stability of SLNs with low and high internal phase proportions. This information will allow to determine if Otoba wax can be used as an ingredient for the preparation of nanometric vehicle systems for cosmetic formulations.

2. Material and Methods

2.1. Materials

Otoba wax was purchased from Drogueria San Jorge (Santiago de Cali, Colombia), and it was used without modifications. Sorbitan oleate (Span^{TM} 80, HLB = 4.3, melting point = 10–12 °C), and polysorbate 80 (Tween^{TM} 80, HLB = 15, melting point = –21 °C) were acquired from CRODA (Snaith, United Kingdom). Methylparaben and propylparaben were purchased from Sigma-Aldrich (St. Louis, MO, USA). Water Type II (ultrapure water) was obtained from a Millipore Elix Essential purification system (Merck KGaA, Darmstadt, Germany).

2.2. Physicochemical Quality Control and Lipid Composition Profile of Otoba Wax

The physicochemical characterization and analyses of the fatty acid methyl ester profiles of the Otoba wax were conducted using methods recommended by the American Oil Chemists' Society (AOCS) [21] and the United States Pharmacopeia (USP) [22]. The determination of the refractive index, saponification value, peroxide value, iodine value, and acid index were, respectively, performed according to the following guidelines: AOCS Cc 7-25, AOCS Cd 3-25, AOCS Cd 8-53, (AOCS Cd 1c-85), and USP 40 <401>. The determination of the fatty acid methyl ester profiles was performed according to AOCS Ce 1-62. To determine the refractive index, a refractometer (VEE GEE Scientific Abbe Model C10, Vernon Hills, IL, USA.) was used. The analysis of fatty acid was conducted using a gas chromatograph (Hewlett Packard HP 5890—Series II, Palo Alto, CA, USA) equipped with a flame ionization detector and a BPX70-ms capillary column (30 m × 0.25 mm × 0.25 μm) composed of 70% cyanopropyl polysilphenylene-siloxane. The initial temperature was 150 °C/min, which was further increased by 5 °C/min up to 240 °C. The injector temperature was 240 °C and the detector temperature was 280 °C (split ratio of 1:30). The carrier gas used was He at 1 mL/min, with a pressure of 11 psi.

2.3. Determination of Required HLB for Otoba Wax

The required HLB value (HLB^r) for Otoba wax was obtained using contact angle and Creaming Index (*CI*) methodologies. In both methods, a surfactant mixture (Tween^{TM} 80 + Span^{TM} 80) in a fixed proportion of 2% *w/w* was employed. The surfactant blend was combined in several proportions, and this process resulted in the different HLB values (8, 9, 10, 11, 12, 13, 14, and 15) of the mixed surfactant (*HLB^M*). This parameter was calculated according to:

$$HLB^M = xHLB_a + (1-x)HLB_b \tag{1}$$

where HLB^M is the value of the binary surfactant blend and HLB_a and HLB_b are the HLB values of the respective surfactants according to their technical sheets.

In the case of the contact angle methodology, the samples were prepared by melting the Otoba wax at 40 °C and by incorporating the surfactant blend. Thereafter, the mixture was solidified at 23 °C, and the measurements were performed on the system surface. By contrast, the CI methodology was conducted using wax-in-water dispersions. These dispersions were prepared using Otoba wax at two internal phase proportions (5 and 20% *w/w*) along with a fixed surfactant mixture of 2% and were dispersed and homogenized using an Ultra-Turrax homogenizer at 5000 rpm for 5 min. Once the dispersions were prepared, the CI was immediately measured.

2.3.1. Contact Angle

Approximately 1 g of sample was spread on a glass slide to form a flat and uniform surface with an area of ~1 cm^2 and a height of ~1 mm. Subsequently, the static contact angle formed between a drop of ultrapure water and the waxy sample surface was measured by the sessile drop method [23]. A contact angle meter (OCA15EC Dataphysics Instruments, Filderstadt, Germany) together with a software controller (Vs. 4.5.14 SCA20) were employed. All measurements were conducted at 22 ± 1 °C and 60% ± 5% relative humidity. Each measurement was conducted in triplicate on different sites of the film surface.

2.3.2. Creaming Index

Freshly made dispersions were added to Falcon™ 15 mL conical centrifuge tubes (diameter = 1.5 cm) and were centrifuged at 3000 rpm (150 RFC) for 4 h in a Wincon 80-2 Centrifuge (Changsha, China). The value of the Creaming Index (*CI*) was determined as follows:

$$CI = \frac{H_S}{H_E} \times 100 \tag{2}$$

where H_S is the sediment height and H_E is the sample height prior to centrifugation.

2.4. Elaboration of SLNs

Coarse dispersions (1200 g) were prepared using Otoba wax at two internal phase proportions (5 and 20% *w/w*). In both cases, ultrapure water, a fixed ratio of surfactant mix of 2%, and a preservative mix of 0.44% were used as the external phase. In the case of the surfactant mix, Tween™ 80 at 1.12% and Span™ 80 at 0.88% were used to provide an HLB^B value of 9. In the preservative mix, methylparaben at 0.30% and propylparaben at 0.14% were included. Both dispersions were made in the same way, in which Otoba wax and ultrapure water were heated to 40 °C. Once the target temperature was achieved, the Span™ 80 surfactant was added to the Otoba wax (premix A), whereas the Tween™ 80 surfactant and the paraben mixture were added to the ultrapure water (premix B). Both premixes were left at the controlled temperature (40 °C) and were stirred (350 rpm) until a homogeneous phase was formed. Subsequently, premix A was added to premix B at 40 °C and was dispersed with a homomixer at 5000 rpm for 5 min. The coarse emulsions were then allowed to cool to room temperature (~23 °C) and were subjected to homogenization by UHPH using a Nano DeBEE Laboratory Homogenizer (BEE International, South Easton, MA, USA). The operating conditions employed were: Zirconia nozzle with an orifice diameter of 0.20 mm, six zirconia reactors with an orifice diameter of 1.75 mm, a pressure of 40,000 psi (2757.9 MPa), and a reverse flow configuration (total of four recirculation cycles). These conditions were previously established by a series of tests that were performed before the formulation of the nanosystems.

2.5. Thermal Stability Assays of SLNs

Each SLNs formulation was placed in a Falcon™ 15 mL conical centrifuge tube, which was subsequently incubated at two temperature conditions: 40 ± 2 °C and 4.0 ± 0.5 °C. The stability test was performed by varying the temperature for 4 weeks. First, the samples were subjected to 40 °C during the first week, 4 °C during the second week, 40 °C during the third week, and finally, 4 °C during the fourth week. The stability parameters that were evaluated included Creaming Index (CI), drop size, viscosity, zeta potential, electrical conductivity, and pH. In the case of CI, the procedure was performed as described in Section 2.3.2.

2.5.1. Particle Size

For the coarse dispersions, droplet size distribution was obtained using a Mastersizer 3000 (Malvern Instruments, Worcestershire, UK) equipped with a helium/neon laser at a wavelength of 632.8 nm, where ~0.6 g of the emulsion was previously diluted with 10 mL of ultrapure water at 25 °C $\pm$ 2 °C and was stirred at 400 rpm prior to the measurement. The appropriate amount of sample was obtained when the obscurance level reached 2–8%. Droplet size data were expressed as $D_{[4,3]}$ [24]. For the SLNs, particle size and polydispersity index (PDI) were determined using a Zetasizer Nano ZSP (Malvern Instrument, Worcestershire, UK) with a red helium/neon laser (633 nm), where 10 μL of each sample was dissolved in 10 mL of distilled water. The particle size was measured using dynamic light scattering with an angle scattering of 173°, using a quartz flow cell (ZEN0023) at 25 °C. The instrument reports particle size as the mean particle diameter (z-average) and a PDI ranging from 0 (monodisperse) to 1 (very broad distribution). All measurements were performed in triplicate.

2.5.2. Viscosity

Viscosity was measured using a viscometer (micro-VISC, RheoSense Inc., San Ramon, CA, USA), applying a shear rate of 7850 s^{-1}. All measurements were performed in triplicate.

2.5.3. Zeta Potential, Electrical Conductivity, and pH

Zeta potential measurements were performed using a Zetasizer Nano ZSP (Malvern Instruments, Worcestershire, UK) at 25 °C $\pm$ 2 °C, with equilibration times of 120 s in a DTS 1070 capillary cell. For these experiments, the attenuator position and intensity were set automatically. The samples were prepared using ~130 mg SLNs, which were diluted in 20 mL of ultrapure water and stirred manually. A 50 μL aliquot was taken and diluted with 1 mL of ultrapure water before each zeta potential measurement. Conversely, the electrical conductivity and the pH were determined using a CR-30 conductivity meter and a Starter-2100 pH meter, respectively. All measurements were performed in triplicate.

2.6. Microbiological Test

The antimicrobial tests for the SLNs were performed according to the microbiological examination of the nonsterile products (tests for specified microorganisms) of USP guidelines [25]. Briefly, total mesophilic aerobes (CFU/g), *Escherichia coli* (CFU/g), Enterobacteriaceae, coagulase-positive *Staphylococcus* (CFU/g), fungi, and yeasts were calculated under the specifications of each microorganism, and the minimal inhibitory concentration (MIC) was visually determined after incubation. In this case, antimicrobial tests were performed for both SLNs with a low and high internal phase. Furthermore, these measurements were performed only for the fourth week of the stability study.

2.7. Graphs and Statistical Analysis

The determination of the average values, standard deviations, and graphs were conducted using the GraphPad Prism 8 software.

3. Results and Discussion

3.1. Physicochemical Quality Control and Lipid Composition Profile of Otoba Wax

As mentioned in the Introduction, Otoba wax is currently being marketed as a raw material or rustic cosmetic product for hair treatment, and information on this material is extremely limited (in conventional databases) and dated [19,26]. Nevertheless, available data regarding the physical characteristics and lipid profile of this wax were very similar to that previously reported (Table 1). The results indicated that Otoba wax consists of a high percentage of saturated fatty acids (89.07%), with lauric (34.67%) and myristic (44.94%) acids as the major components. This result is very interesting because these fatty acids have been reported to provide beneficial effects for hair loss [27,28]. Therefore, Otoba wax could be used as a potential raw material for hair cosmetic products. Moreover, a low composition of unsaturated fatty acids (10.92%) was also found, in which oleic acid (8.24%) and linoleic acid (1.92%) were the primary components. Regarding the physicochemical features, the wax exhibited a melting point of ~34.4 °C, which is a very interesting result for the development of SLNs, because one of the most important physical characteristics is the use of waxes with melting points between 34 °C and 37 °C [8,18]. In contrast, the iodine value (11.2) was consistent with the low amount of unsaturated fats in this wax, whereas the acid index (4.55%) and peroxides (0.30) values suggest that the Otoba wax used in this study does not have the required characteristics to be considered as a premium raw material. These results are consistent considering the rustic and low-tech way in which this wax is usually obtained.

Table 1. Results of physicochemical quality control and the composition of fatty acid methyl ester profiles of Otoba wax.

Profile of Lipid Composition (Saturated Fatty Acids)			
Common Name	**IUPAC Name**	**Shorthand**	**Value (%)**
Caproic acid	Hexanoic acid	6:0	0.01
Caprylic acid	Octanoic acid	8:0	0.96
Capric acid	Decanoic acid	10:0	1.00
Lauric acid	Dodecanoic acid	12:0	34.67
Myristic acid	Tetradecanoic acid	14:0	44.94
Pentadecylic acid	Pentadecanoic acid	15:0	0.02
Palmitic acid	Hexadecanoic acid	16:0	5.72
Stearic acid	Octadecanoic acid	18:0	1.42
Arachidic acid	Icosanoic acid	20:0	0.24
Behenic acid	Docosanoic acid	22:0	0.05
Lignoceric acid	Tetracosanoic acid	24:0	0.04
		Total:	**89.07**
Profile of Lipid Composition (Unsaturated Fatty Acids)			
Common Name	**IUPAC Name**	**Shorthand**	**Value (%)**
Palmitoleic acid	(Z)-hexadec-9-enoic acid	16:1n-7	0.07
Oleic acid	(Z)-octadec-9-enoic acid	18:1n-9	8.24
Linoleic acid	(9Z,12Z)-octadeca-9,12-dienoic acid	18:2n-6	1.92
α-Linolenic acid	(9Z,12Z,15Z)-octadeca-9,12,15-trienoic acid	18:3n-3	0.07
Gadoleic acid	(Z)-icos-9-enoic acid	20:1n-11	0.62
		Total:	**10.92**
Physicochemical Parameter		**Value**	
Melting point (°C)		34–35	
Refractive index		1.418 (20 °C) and 1.4720 (40 °C)	
Saponification value (mg KOH/g)		235.56	
Peroxide value (meq O/kg)		0.30	
Iodine value (g I_2/100 g)		11.2	
Acid index (% oleic acid)		4.55	

3.2. Determination of the Required HLB for Otoba Wax

Figure 1A shows the contact angle formed between the Otoba wax surface (nonpolar phase) and ultrapure water (polar phase) at two internal phase ratios in the absence (control) and presence of neutral surfactants (Tween[TM] 80 + Span[TM] 80) with different HLB[M] values. The results indicated that the lowest contact angle value is reached when the HLB[M] value is 9. Therefore, this specific proportion of surfactants is one that leads to the maximum decrease in the hydrophobic effect [29] generated between both phases. This behavior was also observed for the Creaming Index in both internal phase proportions (Figure 1B), where the minimum value was achieved with an HLB[M] of 9. These results suggest that it is necessary to use a mixture of neutral surfactants with an HLB[M] of ~9 to achieve the maximum decrease in the interfacial tension between Otoba wax and ultrapure water and to form a compact surfactant layer around the waxy particle. Therefore, the required HLB value for Otoba wax was such value, which was considered for the development of SLNs in both internal phase proportions.
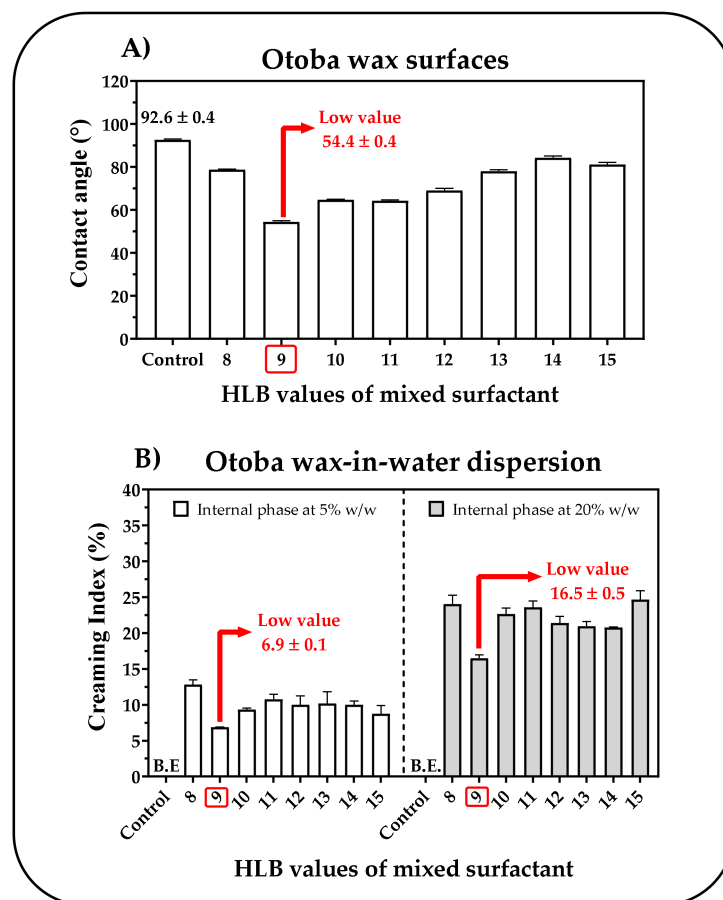
Figure 1. (**A**) Contact angle of Otoba wax surfaces and (**B**) Creaming Index of Otoba wax-in-water dispersion, in the absence and presence of Span[TM] 80 + Tween[TM] 80 for different HLB values of mixed surfactants.

3.3. Thermal Stability Assays of SLNs

A significant aspect to highlight is that both SLNs formulations (low and high internal phases) were formulated at a low emulsifier proportion (2%). Therefore, the results obtained for the thermal stability assays depended exclusively on the UHPH process and not on other factors. Figures 2 and 3 show the thermal stability results, and these results are discussed below according to each evaluated parameter.
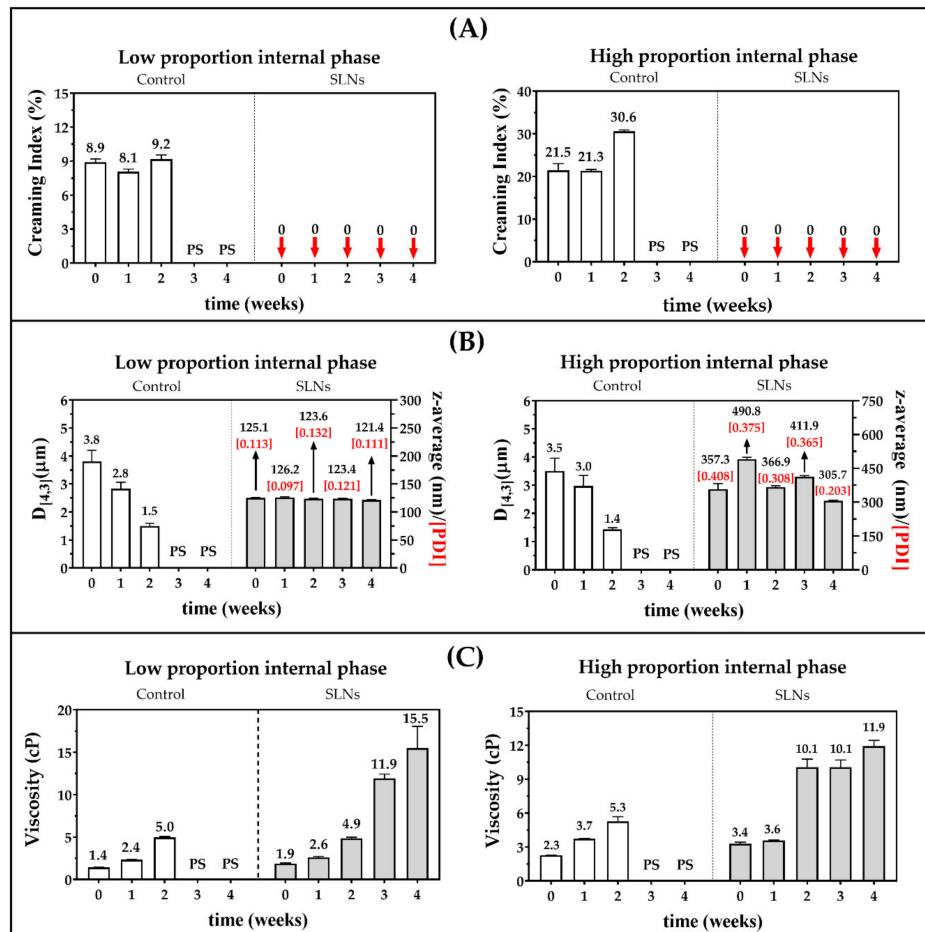
Figure 2. (**A**) Creaming Index (CI), (**B**) droplet size ($D_{[4,3]}$), z-average and polydispersity index (PDI), and (**C**) viscosities of solid lipid nanoparticles (SLNs) dispersed in ultrapure water at different times of thermal stability. PS indicates that there is no value due to the phase separation (some pictures about the emulsified and nanoemulsified systems at the zero and final times are shown in the Supplementary Material file).
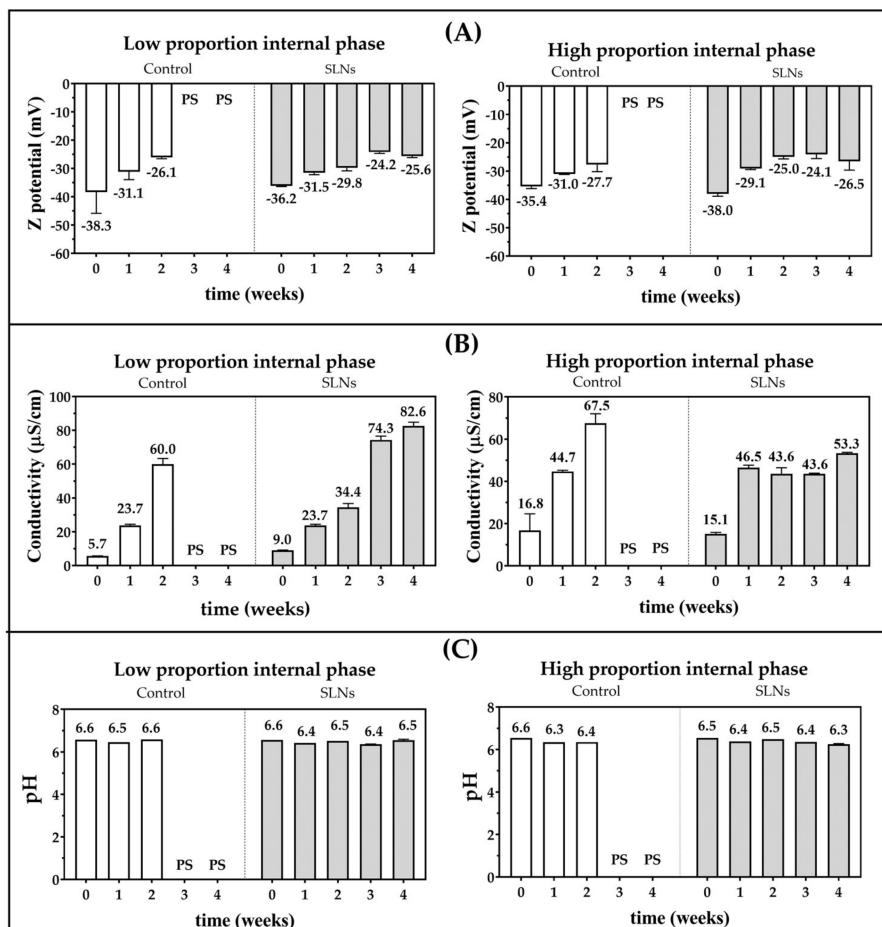
Figure 3. (**A**) Zeta potential, (**B**) electrical conductivity, and (**C**) pH of solid lipid nanoparticles (SLNs) dispersed in ultrapure water at different times of thermal stability. PS indicates that there is no value due to the phase separation.

3.3.1. Creaming Index (CI)

Figure 2A shows that after the second week of the thermal study, the controls corresponding to those systems not subjected to UHPH exhibited phase separation, indicating a progressive decrease in the physical stability of the heterodispersed system. Likewise, the CI values are higher in those systems with a high internal phase proportion, which is consistent, because the stabilizing surfactant amount is 10-fold less than that of systems with a low internal phase (2.5-fold). By contrast, SLNs subjected to UHPH did not show any change in CI value, thus suggesting that they had greater physical stability. This result is consistent with the UHPH methodology employed, in which a high shear energy was applied, thus leading to the formation of dispersed systems with very small particle sizes and low polydispersity [30]. These characteristics demonstrate that the SLNs developed by UHPH avoid the fast aggregation process between dispersed solid lipid particles and provide greater physical stability [5].

3.3.2. Particle Size

Figure 2B shows that the particle size for both controls decreased over time, whereas the SLNs exhibited a different behavior, similar to those observed in the CI assays. This suggest that UHPH produces a new configuration in the heterodispersed system. Furthermore, the effects of shear, cavitation, and impact generated during the process led to a notable decrease in the internal phase of SLNs, along with high uniformity. Regarding the controls, the results obtained are very interesting, because this parameter is usually expected to increase over time due to the dispersed particle aggregation process; however, it was the opposite. This result could be explained by considering that

the particle size ($D_{[4,3]}$) is a mean value, and therefore, the system consists of particles with different sizes (small, medium, and large) [24]. Hence, when the thermal study begins, a dynamic movement of the surfactants occurs, in which they are desorbed from the interfaces of the largest particles that subsequently form aggregates, leaving only the small particles. Similarly, this surfactant desorption also explains why the creaming formation is greater in the controls than in the systems subjected to UHPH. By contrast, the SLNs exhibited a low internal phase, and the particle size (z-average) remained practically unchanged (~125 nm) with low polydispersity (<0.3). In those with high internal phase, the z-average was greater and fluctuated between ~350 and ~500 nm, and the polydispersity decreased from ~0.4 to ~0.2 over time. This result is consistent because in such a system, the surfactant amount is very low compared with the amount of the waxy dispersed phase. Furthermore, the surfactant layer that surrounds the waxy particle may not be well formed compared with the low internal phase systems. Nevertheless, this problem could be improved by increasing the surfactant amount in such a formulation with a high internal phase. Likewise, the polydispersity decreases in these SLNs, thus suggesting that the dispersed wax phase tends to become more organized over time.

3.3.3. Viscosity

In relation to the viscosity, Figure 2C shows that it increased over time, both in the controls and in the SLNs. After the second week, this parameter increased considerably. In the case of the controls, the viscosity described a behavior that is very similar to each other in the first 2 weeks, where viscosity in the low and high internal phase systems increased from 1.4 to 5.0 and from 2.3 to 5.3, respectively. Regarding SLNs viscosity, they also describe a similar behavior, where viscosity in the low and high internal phase systems increased from 1.9 to 15.5 and from 3.4 to 11.9, respectively. This finding indicates that the viscosity is higher in systems with small particle sizes and low polydispersity. These results are similar to those previously observed for CI and particle size, where the UHPH resulted in a relatively steady state. Therefore, this condition leads to a decrease in the aggregation phenomena (e.g., flocculation, coalescence, and cremation) and where the dispersed phase self-organizes, forming networks between the surfactant layer and the aqueous medium, thus increasing cohesiveness and system viscosity.

3.3.4. Zeta Potential, Electrical Conductivity, and pH

The results of zeta potential assays for the heterodispersed systems at different times and with different process conditions are shown in Figure 3A, which are very interesting because the stabilizer surfactants utilized (Tween^{TM} 80 and Span^{TM} 80) are neutral, and therefore, the expected values should be close to zero. However, all the zeta potential values obtained were negative. These results can be explained by the spontaneous formation of a tiny monolayer of hydroxyl ions at the wax–surfactant–water interface, resulting from autoprotolysis of water [31,32]. Likewise, it was observed that SLNs and their respective controls showed a decrease in the zeta potential with respect to time. This result could be explained by the previously mentioned results for CI, particle size, and viscosity. Therefore, in the case of control, it may be considered that such a decrease is given by the desorption of the surfactants, in which the interface of the dispersed phase is depolarized. In SLNs, the zeta potential decreases because the electric double layer is compressed by the increase in the system viscosity [33].

The results of electrical conductivity are shown in Figure 3B and are attributed to the presence of hydronium and hydroxyl ions from the autoprotolysis of water, the ions possibly formed from ionization of the paraben preservatives and the small amounts of carbonic acid that can be generated in situ between CO_2 and the dispersing aqueous phase. Furthermore, it was found that the controls and the SLNs displayed a similar trend, in which conductivity increased proportionally with time. However, in the SLNs with a high internal phase, conductivity reached a slightly fluctuating range of values from the first week of the study. Similarly, it can be observed that when the electrical conductivity increased, the zeta potential decreased and the SLNs with a lower internal phase exhibited

higher conductivity values than those with a higher internal phase. These results can be explained by considering that a reorganization of the electrical double layer in the dispersed particles occurs over time. Therefore, the ions located in this layer move toward bulk, acquiring better electrical mobility and a larger conductivity.

Figure 3C shows the results regarding pH. It was found that the control and the SLNs exhibited very similar pH values between 6.3 and 6.6. These acidic values can be attributed to two factors, namely, (i) the chemical nature of some ingredients utilized in the formulation and (ii) the acidification of the dispersing phase by the formation of carbonic acid. In the first case, the preservatives used were the alkyl esters of p-hydroxybenzoic acid, which has a phenol substituent that can be ionized and decrease the pH of the dispersing phase. In contrast, the dispersion process of the waxy phase in the aqueous phase can lead to the incorporation of air bubbles that contain CO_2 (g) which is transformed to carbonic acid after coming into contact with water [34]. This effect is shown by the change in pH of two ultrapure water samples, in which one was subjected to Ultra-Turrax, whereas the other was not. The results were convincing because it was found that the sample of water subjected to Ultra-Turrax exhibited a more acidic pH than the sample not subjected.

Although some degradation effect could also be considered regarding the surfactants employed or with the esterified fats present in the wax, their degree of hydrophobicity would limit such a process. Therefore, the acid values observed are exclusively attributed to the ionization of the preservatives used and, to a lesser degree, the formation of carbonic acid.

3.4. Microbiological Test

The results of the microbiological test for the Otoba wax SLNs developed by UHPH are summarized in Table 2. It was found that each one of these systems met the quality specifications defined for the tested microorganisms. The results were consistent, because two model preservatives were included in these formulations, which were well known to provide high microbiological stability. Therefore, it is possible to ensure that the changes observed during the stability study were exclusively due to the intrinsic nature of the formulation and the process conditions used.

Table 2. Results of the antimicrobial tests for the solid lipid nanoparticles (SLNs).

SLNs	Microorganism Tested					
	Mesophilic Aerobes (CFU/g)	*Escherichia coli* (CFU/g)	Enterobacteriaceae	Coagulase-positive *Staphylococcus* (CFU/g)	Fungi	Yeasts
Low internal proportion	<10	Absent	Absent	Absent	Absent	<10
High internal proportion	69	Absent	Absent	Absent	Absent	36

4. Conclusions

Otoba wax is described as a lipid composition that consist mainly of lauric (~35%) and myristic (~45%) acids. It is a promising raw material for the hair cosmetics sector, because it has been reported that its components can ameliorate hair loss. Otoba wax has a melting point of 34.7 °C, therefore, it can be used for the development of SLNs. However, it is found that several physicochemical characteristics of this wax, such as the acid index and peroxide value, are high; therefore, it cannot be considered a premium raw material. Consequently, it is necessary to improve, standardize, and establish technical methods for processing this wax. In addition, it was found that the required HLB for Otoba wax was around 9. Regarding to the development of heterodispersed systems, it was found that different physical characteristics may be acquired depending on the amount of internal phase used and its submission to UHPH. If the systems are not subjected to UHPH (controls), they may have large particle

sizes and become unstable, even after using surfactants with an HLB^M equal to the required HLB for such a wax. In contrast, the systems developed by UHPH achieved high stability against aggregation and cremation, in which particle size, polydispersity, and zeta potential decreased over time in thermal studies, whereas viscosity and conductivity increased. Finally, the Otoba wax and the UHPH proved to have a high potential for the development of nanometric hair cosmetic formulations.

Author Contributions: Methodology and investigations, S.R. and J.D.E.; supervision, writing, reviewing, and editing, C.H.S. All authors have read and agreed to the published version of the manuscript.

Conflicts of Interest: The authors declare no conflict of interests.

References

1. Yadav, N.; Khatak, S.; Singh Sara, U.V. Solid lipid nanoparticles—A review. *Int. J. Appl. Pharm.* **2013**, *5*, 8–18.
2. Radomskasoukharev, A. Stability of lipid excipients in solid lipid nanoparticles. *Adv. Drug Deliv. Rev.* **2007**, *59*, 411–418. [CrossRef] [PubMed]
3. Garud, A.; Singh, D.; Garud, N. Solid Lipid Nanoparticles (SLN): Method, Characterization and Applications. *Int. Curr. Pharm. J.* **2012**, *1*, 384–393. [CrossRef]
4. Poliseli-Scopel, F.H.; Hernández-Herrero, M.M.; Guamis, B.; Ferragut, V. Comparison of ultra high pressure homogenization and conventional thermal treatments on the microbiological, physical and chemical quality of soymilk. *LWT* **2012**, *46*, 42–48. [CrossRef]
5. Rave, M.C.; Echeverri, J.D.; Salamanca, C.H. Improvement of the physical stability of oil-in-water nanoemulsions elaborated with Sacha inchi oil employing ultra-high-pressure homogenization. *J. Food Eng.* **2020**, *273*, 109801. [CrossRef]
6. Ganesan, P.; Narayanasamy, D. Lipid nanoparticles: Different preparation techniques, characterization, hurdles, and strategies for the production of solid lipid nanoparticles and nanostructured lipid carriers for oral drug delivery. *Sustain. Chem. Pharm.* **2017**, *6*, 37–56. [CrossRef]
7. Dumay, E.; Chevalier-Lucia, D.; Picart-Palmade, L.; Benzaria, A.; Grácia-Juliá, A.; Blayo, C. Technological aspects and potential applications of (ultra) high-pressure homogenisation. *Trends Food Sci. Technol.* **2013**, *31*, 13–26. [CrossRef]
8. Pardeshi, C.; Rajput, P.; Belgamwar, V.; Tekade, A.; Patil, G.; Chaudhary, K.; Sonje, A. Solid lipid based nanocarriers: An overview/Nanonosači na bazi čvrstih lipida: Pregled. *Acta Pharm.* **2012**, *62*, 433–472. [CrossRef]
9. Bunjes, H. Lipid nanoparticles for the delivery of poorly water-soluble drugs. *J. Pharm. Pharmacol.* **2010**, *62*, 1637–1645. [CrossRef]
10. Müller, R.H.; Mäder, K.; Gohla, S. Solid lipid nanoparticles (SLN) for controlled drug delivery—A review of the state of the art. *Eur. J. Pharm. Biopharm.* **2000**, *50*, 161–177. [CrossRef]
11. Kalhapure, R.S.; Suleman, N.; Mocktar, C.; Seedat, N.; Govender, T. Nanoengineered Drug Delivery Systems for Enhancing Antibiotic Therapy. *J. Pharm. Sci.* **2015**, *104*, 872–905. [CrossRef] [PubMed]
12. Naseri, N.; Valizadeh, H.; Zakeri-Milani, P. Solid Lipid Nanoparticles and Nanostructured Lipid Carriers: Structure, Preparation and Application. *Adv. Pharm. Bull.* **2015**, *5*, 305–313. [CrossRef] [PubMed]
13. Wissing, S.; Kayser, O.; Müller, R. Solid lipid nanoparticles for parenteral drug delivery. *Adv. Drug Deliv. Rev.* **2004**, *56*, 1257–1272. [CrossRef] [PubMed]
14. Durán-Lobato, M.; González, A.E.; Arevalo, M.F.; Martín-Banderas, L. Statistical analysis of solid lipid nanoparticles produced by high-pressure homogenization: A practical prediction approach. *J. Nanopart. Res.* **2013**, *15*, 1443. [CrossRef]
15. Müller, R.; Radtke, M.; Wissing, S. Solid lipid nanoparticles (SLN) and nanostructured lipid carriers (NLC) in cosmetic and dermatological preparations. *Adv. Drug Deliv. Rev.* **2002**, *54*, S131–S155. [CrossRef]
16. Weiss, J.; Decker, E.A.; McClements, D.J.; Kristbergsson, K.; Helgason, T.; Awad, T. Solid Lipid Nanoparticles as Delivery Systems for Bioactive Food Components. *Food Biophys.* **2008**, *3*, 146–154. [CrossRef]

17. Wissing, S. Cosmetic applications for solid lipid nanoparticles (SLN). *Int. J. Pharm.* **2003**, *254*, 65–68. [CrossRef]

18. Müller, R.; Petersen, R.; Hommoss, A.; Pardeike, J. Nanostructured lipid carriers (NLC) in cosmetic dermal products. *Adv. Drug Deliv. Rev.* **2007**, *59*, 522–530. [CrossRef]

19. Bhacca, N.S.; Stevenson, R. The Constitution of Otobain. *J. Org. Chem.* **1963**, *28*, 1638–1642. [CrossRef]

20. Lopez Tobar, R.; Neill, D.; Torres, B.; Guerra, D. El Doncel (*Otoba parvifolia*) en Napo Napumanta wapa yura (*Otoba parvifolia*). *Huellas del Sumaco Revista Socio Ambiental de la Amazonía Ecuatoriana* **2014**, *12*, 1.

21. *American Oil Chemists' Society Official Methods and Recommended Practices*; AOCS: Champaign, IL, USA, 2017.

22. USP <191> Identification Tests—General. United State Pharmacopeial. Available online: https://www.uspnf.com/notices/usp-nf-online-gc-191-pub-correction (accessed on 3 June 2020).

23. Kwok, D.; Neumann, A. Contact angle measurement and contact angle interpretation. *Adv. Colloid Interface Sci.* **1999**, *81*, 167–249. [CrossRef]

24. Liu, W.; Pi, S. AC magnetic nanothermometry: The influence of particle size distribution. In Proceedings of the 2016 10th International Conference on Sensing Technology (ICST), Nanjing, China, 11–13 November 2016; Institute of Electrical and Electronics Engineers (IEEE): Piscataway, NJ, USA, 2016; pp. 1–3.

25. USP <61> Microbiological examination of Nonsterile Products: Microbial Enumeration Tests. Available online: https://www.usp.org/sites/default/files/usp/document/harmonization/gen-method/q05b_pf_ira_34_6_2008.pdf (accessed on 3 June 2020).

26. Baughman, W.F.; Jamieson, G.S.; Brauns, D.H. An analysis of otoba butter. *J. Am. Chem. Soc.* **1921**, *43*, 199–204. [CrossRef]

27. Mccoy, J.; Ziering, C.; Biology, A.; Ste, F. Botanical Extracts for the Treatment of Androgenetic Alopecia. *Int. J. Life Sci. Pharma Res.* **2012**, *2*, 31–38.

28. Dhariwala, M.; Ravikumar, P. An overview of herbal alternatives in androgenetic alopecia. *J. Cosmet. Dermatol.* **2019**, *18*, 966–975. [CrossRef] [PubMed]

29. Kronberg, B.; Costas, M.; Silvestonti, R. Understanding the hydrophobic effect. *J. Dispers. Sci. Technol.* **1994**, *15*, 333–351. [CrossRef]

30. Zamora, A.; Ferragut, V.; Jaramillo, P.; Guamis, B.; Trujillo, A.-J. Effects of Ultra-High Pressure Homogenization on the Cheese-Making Properties of Milk. *J. Dairy Sci.* **2007**, *90*, 13–23. [CrossRef]

31. Gao, P.; Xing, X.; Li, Y.; Ngai, T.; Jin, F. Charging and discharging of single colloidal particles at oil/water interfaces. *Sci. Rep.* **2014**, *4*, 4. [CrossRef]

32. Marinova, K.; Alargova, R.G.; Denkov, N.D.; Velev, O.D.; Petsev, D.N.; Ivanov, I.B.; Borwankar, R.P. Charging of Oil–Water Interfaces Due to Spontaneous Adsorption of Hydroxyl Ions. *Langmuir* **1996**, *12*, 2045–2051. [CrossRef]

33. Hunter, R.J. *Zeta Potential in Colloid Science: Principles and Applications*; Academic Press: Cambridge, MA, USA, 2013; ISBN 9781483214085.

34. Mook, W.G. Chemistry of carbonic acid in water. In *Environmental Isotopes in the Hydrological Cycle*; International Atomic Energy Agency and United Nations Educational, Scientific and Cultural Organization: Amsterdam, The Netherlands, 2000.